



Royal Netherlands
Meteorological Institute
Ministry of Infrastructure and the
Environment

The EUMETSAT
Network of
Satellite
Application
Facilities



Ocean and Sea Ice SAF

ASCAT-B NWP Ocean Calibration and Validation

**Technical Report
SAF/OSI/CDOP2/KNMI/TEC/RP/199
Products OSI-102-b and OSI-104-b**

**Jeroen Verspeek
Anton Verhoef
Ad Stoffelen**

March 2013

Summary

On September 17, 2012 the Metop-B satellite with onboard the Advanced Scatterometer (ASCAT-B) has been successfully launched. For the ASCAT-B scatterometer, corrections are derived with the use of the NWP ocean calibration (NOC). These corrections are used in the ASCAT wind data processor in order to obtain high-quality winds. The NOC-calibrated ASCAT-B wind product is examined and its quality appears on the same level as that of the ASCAT-A wind product.

Contents

Summary	2
1 Introduction	4
2 NWP Ocean Calibration.....	5
3 NOC correction factors	6
3.1 ASCAT-B ocean calibration	6
3.2 Verification of the NOC correction factors.....	8
4 Visualisation.....	10
5 MLE.....	12
6 Wind statistics	16
7 Quality control.....	19
8 ASCAT-A and ASCAT-B collocation.....	22
9 Buoy validation and triple collocations.....	24
10 Conclusions	26
Glossary.....	28
References	28

1 Introduction

The Metop-B satellite with onboard the Advanced Scatterometer (ASCAT) has been successfully launched on September 17, 2012. ASCAT is a vertically-polarized C-band real-aperture radar with three fan beam antennas pointing to the left-hand side of the sub-satellite track and three fan-beam antennas pointing to the right-hand side [Figa-Saldaña et al, 2002]. ASCAT-B onboard Metop-B is identical to the already operational scatterometer ASCAT-A onboard Metop-A which was launched in 2006.

Within the framework of the Ocean & Sea Ice (OSI) Satellite Application Facility (SAF), KNMI has developed an ocean calibration method, based on Numerical Weather Prediction (NWP) wind inputs, the so-called NWP Ocean Calibration (NOC). The NOC method [Verspeek et al, 2012; Stoffelen, 1999] resides in direct comparison of measured backscatter data with simulated backscatter data from NWP winds using a forward model or Geophysical Model Function (GMF). For ASCAT-A, the CMOD5.n GMF [Hersbach et al, 2010] is used, which is compliant with the GMF of its predecessor, the European Remote-sensing Satellite (ERS) scatterometer [Attema 1991]. However, outer swath backscatter values of the fore and aft beam are extrapolated w.r.t. ERS and an incidence-angle dependent correction to CMOD5.n has been established with ASCAT-A.

The radar backscatter triplets can be visualized in a 3-dimensional measurement space. For a given Wind Vector Cell (WVC), i.e., position across the swath, the measured triplets are distributed around the GMF, which constitutes a well-defined conical surface that depends on wind speed and wind direction only [Stoffelen and Anderson, 1997]. Systematic displacements of the cloud of triplets in any direction of the 3D space are mainly due to absolute beam biases, which are adequately removed by the results of the NOC [Verspeek et al, 2012].

The NOC method has the advantage over other calibration methods (e.g., transponders, rain forest, ice) that it can be applied over a large global area (all the oceans) that provides a substantial amount of data and thus more accurate results over a relatively short period of time. It is therefore also very suitable for monitoring purposes. Here, NOC corrections are derived from and subsequently applied to ASCAT-B data. Then the resulting level 2 products are analysed and, also, analysis using collocated ASCAT-A and ASCAT-B is performed.

In section 2 the NWP ocean calibration method is explained. Section 3 describes the derivation of the NOC corrections for ASCAT-B. For the remaining sections ASCAT data from 2012-11-15 to 2012-11-30 is used. Section 4 shows the visualisation of ASCAT-B data in measurement space. Section 5 validates the statistical characteristics of the inversion residual or MLE [Portabella et al, 2012], section 6 the wind statistics and section 7 the ASCAT-B product quality flags. Section 8 shows the analysis of collocated ASCAT-A and ASCAT-B data and section 9 contains the results of buoy validations and triple collocations. Finally section 10 provides the conclusions.

2 NWP Ocean Calibration

The NOC technique [Stoffelen, 1999] is used to assess the difference between scatterometer backscatter data and simulated backscatter data out of collocated NWP winds using the GMF. Discrepancies between mean measured and simulated backscatter may be due to instrument calibration, systematic and random errors in NWP wind speed and direction and GMF errors. These sources of error should therefore be analyzed carefully. The NOC method is based on the analysis of a large measurement dataset to estimate Fourier coefficients that can be directly compared to those in the CMOD5.n GMF. For any particular WVC in any beam the incidence angle is virtually constant around the orbit and we can model the backscatter with

$$\sigma_0(v, \phi) = B_0(v)[1 + B_1(v) \cos \phi + B_2(v) \cos(2\phi)]^{1.6}$$

where v is wind speed and ϕ is wind direction with respect to the beam pointing direction. The mean backscatter is essentially determined by the value of B_0 with contributions from B_1 and B_2 . In z -space, where $z = \sigma_0^{0.625}$, this becomes

$$z(v, \phi) = \frac{1}{2} a_0(v) + a_1(v) \cos \phi + a_2(v) \cos(2\phi)$$

where $a_0 = 2B_0^{0.625}$, $a_1 = B_1B_0^{0.625}$ and $a_2 = B_2B_0^{0.625}$. Integrating uniformly over azimuth angle gives

$$\frac{1}{2\pi} \int_0^{2\pi} z(v, \phi) d\phi = \frac{1}{2} a_0(v)$$

So, when the wind direction distribution is sampled uniformly for all wind speeds, then the mean of $2a_0$ should be identical to the mean of z . This means that uncertainties in a_1 and a_2 do not contribute to the error in the simulated mean z .

To arrange for a uniform wind direction distribution at each wind speed, we split the data into wind speed bins and azimuth angle bins. Bins are defined such that they are large enough to contain a certain minimum number of measurements and small enough to provide a good approximation of the integral. In the following, indices i and j refer to wind speed bin i and azimuth angle bin j respectively. Index k is used to refer to an individual measurement z_k . Parameters I , J and K refer to the total number of bins or measurements, so $i=1, 2, \dots, I$, $j=1, 2, \dots, J$ and $k=1, 2, \dots, K(i,j)$.

The mean z in a fixed wind speed row is, let's call this $z(i)$:

$$z(i) = \frac{1}{J} \sum_{j=1}^J \frac{1}{K(i,j)} \sum_{k=1}^{K(i,j)} z_k(i,j)$$

Summation over the wind speed rows gives

$$\langle z \rangle = \frac{1}{KJI} \sum_{i=1}^I KJ(i)z(i)$$

with

$$KJ(i) = \sum_{j=1}^J K(i, j), \quad KJI = \sum_{i=1}^I KJ(i)$$

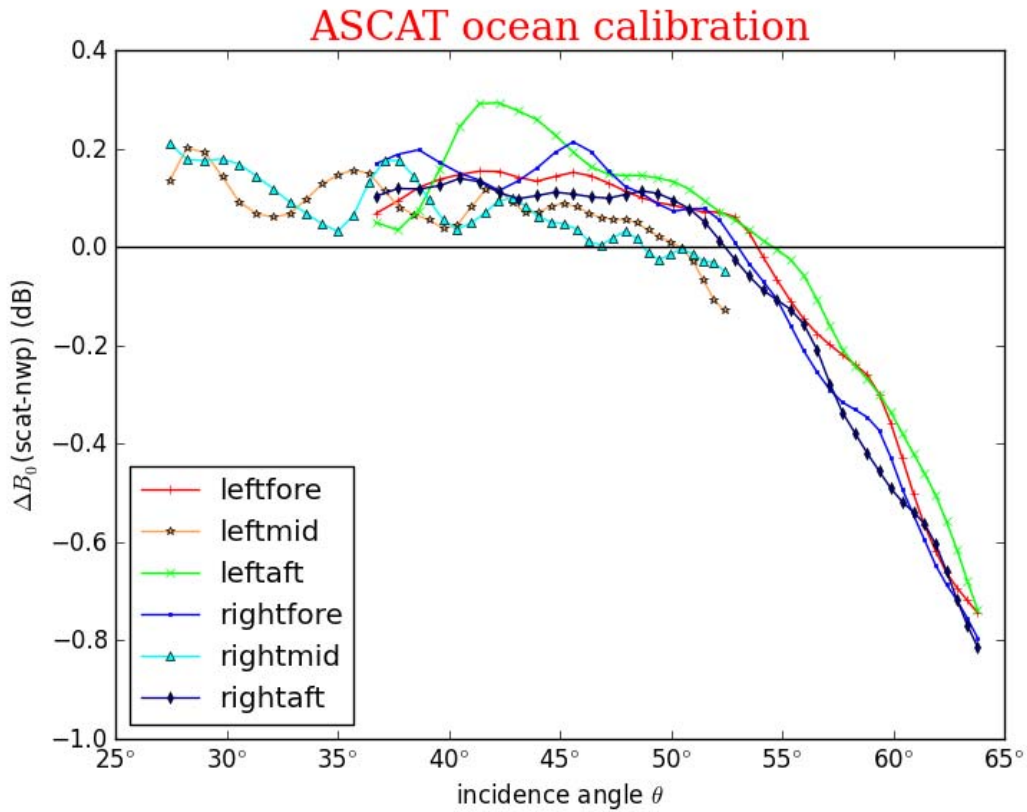
$\langle z \rangle$ is the mean backscatter value over all speeds at a uniform wind direction distribution and may be either measured or simulated by collocated NWP wind inputs and the GMF, where mainly the term as given by $a_0(v)$ or $B_0(v)$ contributes. Any discrepancy between the simulated and measured mean backscatter values is computed as a ratio. A ratio not equal to one may be related to inaccuracies in the instrument gain, e.g., beam pattern determination, or to errors in the NWP input winds and GMF. Here, we use the NOC to correct for instrument gain and validate its effects.

The NWP and GMF related errors slightly decrease with enhanced sampling over all seasons and are estimated to be within 0.1 dB for a one-year calibration period [Verspeek, 2012; Stoffelen, 1999]. This method needs only a few days of collocated ASCAT data and ECMWF winds to produce a reasonable estimate of difference in a_0 within 0.2 dB. We use CMOD5.n with the ECMWF equivalent neutral 10-meter winds to calculate collocated model backscatter values corresponding to the measured values and apply the process as described above. The ratio of the two values of a_0 then provides an estimate of the mean difference between model and measurement backscatter, i.e., instrument gain.

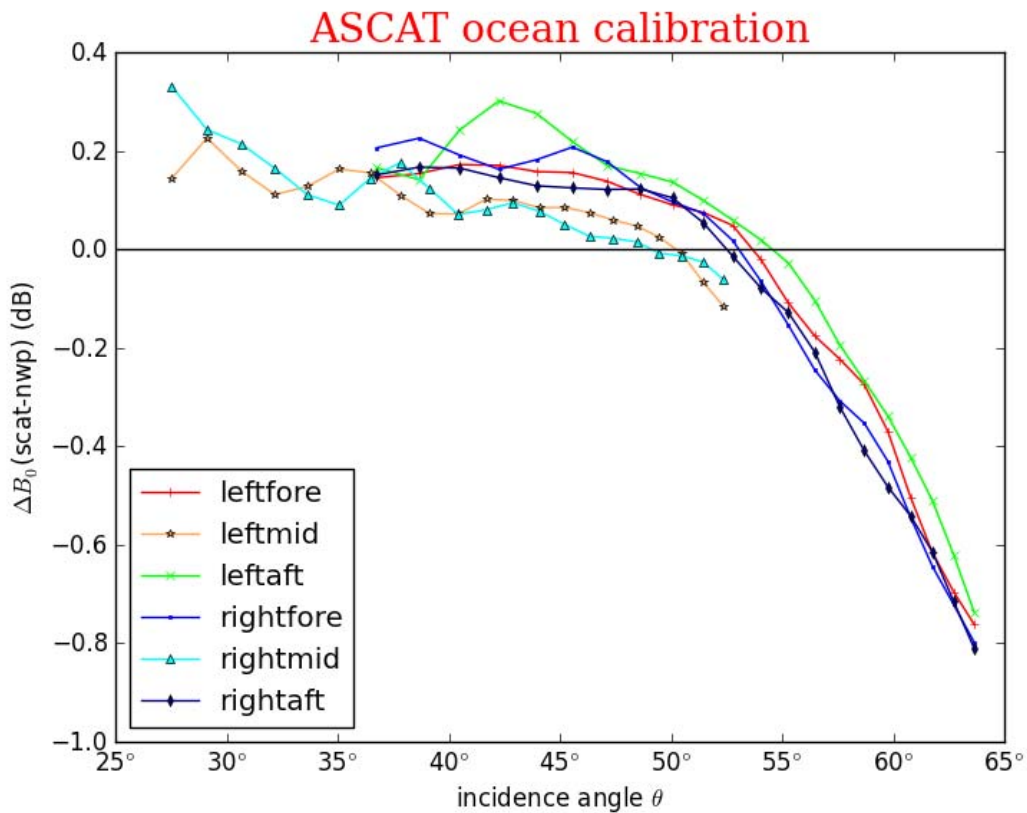
3 NOC correction factors

3.1 ASCAT-B ocean calibration

The ocean calibration is performed on ASCAT-B data over a period of nine days from 2012-10-29 to 2012-11-06 for both the coastal (12.5 km WVC spacing with box filtering) and the 25.0 km product (with Hamming window filtering). These data are all from level-1b software version 8.01. The data is quality controlled and a conservative lat-lon filter is applied in order to rule out possible sea-ice contamination. The resulting pattern in Figure 1a) (coastal product) is similar to what is obtained for ASCAT-A. CMOD5.n uses neutral winds whereas the ECMWF winds are real 10-m winds. Therefore a correction of 0.2 m/s is added to the ECMWF winds in order to compensate for the difference between neutral winds and 10-m winds [Portabella and Stoffelen, 2009]. For high incidence angles the figure shows a decrease of the residuals from about +0.1 dB to -0.8 dB. This pattern is also observed for ASCAT-A. Also wiggles in each of the antenna residuals are present as is the case for ASCAT-A. In fact the wiggle-pattern of ASCAT-B resembles the pattern of ASCAT-A. The residuals shown will be used as NOC correction factors in AWDP. The pattern in Figure 1b) for the 25.0 km product is similar to that in Figure 1a) but some of the details are smeared out due to the coarser resolution.



a)



b)

Figure 1 – Average of the NWP ocean calibration residuals of ASCAT-B over the period 2012-10-29 to 2012-11-06 for a) 12.5 km WVC spacing (coastal product) and b) 25.0 km WVC spacing.

3.2 Verification of the NOC correction factors

In order to verify that NOC correction factors are implemented correctly, a NOC over the same period from 20121029-20121106 is performed. Figure 2 shows the residuals from this run. Indeed the remaining residuals are almost zero.

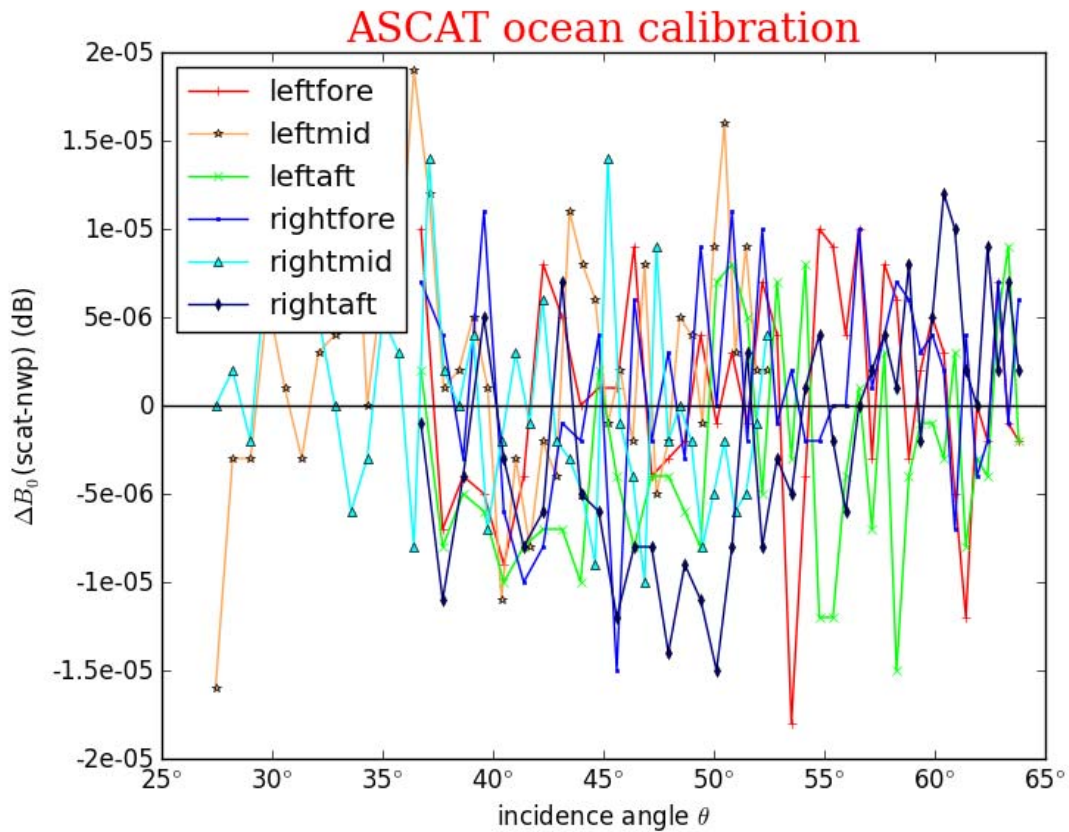


Figure 2 – Nulltest, NOC residuals for ASCAT-B coastal product from 2012-10-29 to 2012-11-06. The NOC corrections were derived from the same dataset.

Figure 3 shows NOC residuals for ASCAT-B data from 2012-11-15 to 2012-11-30 with NOC corrections applied. This period is different from the period the NOC corrections were derived from and thus gives an independent check. These data are used for the remainder of this document. The residuals range from -0.1dB to +0.05 dB which is in the same order as observed for ASCAT-A over independent periods [Verspeek et al, 2012].

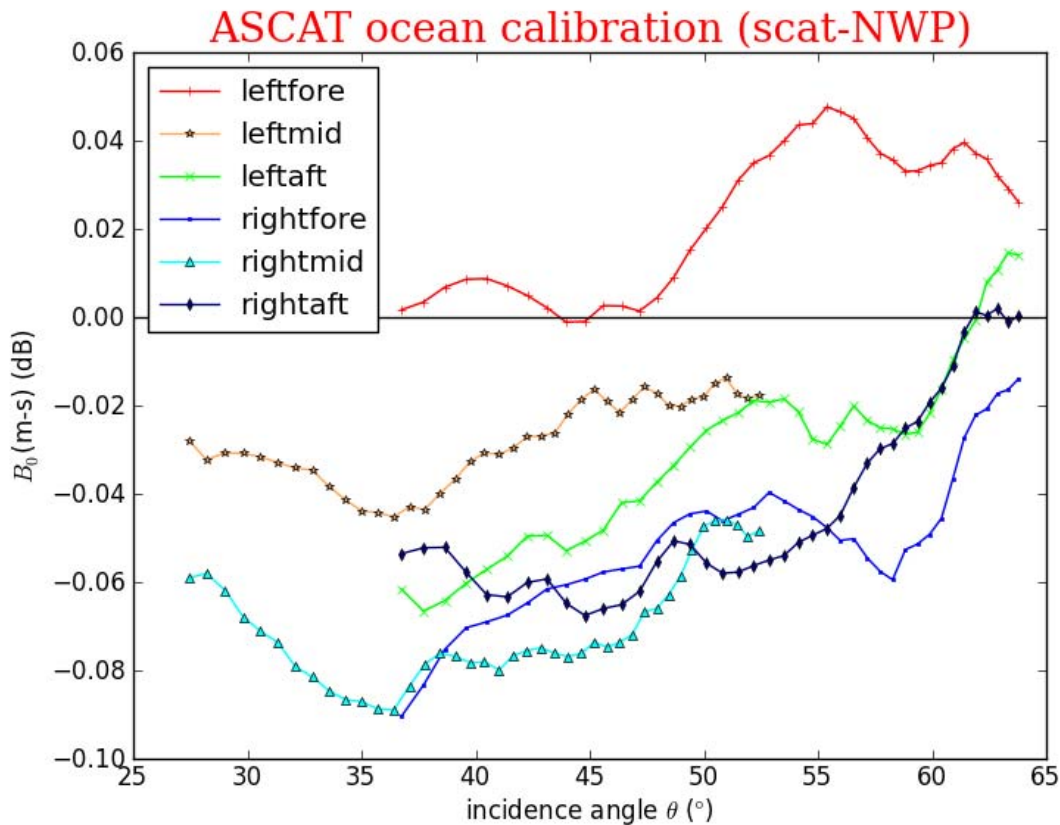


Figure 3 – NOC residuals for ASCAT-B coastal product from 2012-11-15 to 2012-11-30. NOC corrections are applied.

Figure 4 shows the ASCAT-B minus ASCAT-A residuals from an NOC run without NOC corrections with data from 2012-11-15 to 2012-11-30 (double difference). Calibration or instrumental differences between the two scatterometers would show up in this plot given that the sampled weather is very similar indeed. Only relatively small differences in the range of -0.15 dB to +0.15 dB are found.

We further ran the ASCAT-A NOC over the same period as the ASCAT-B NOC and verified its close proximity to the ASCAT-A calibration used in AWDP (not shown). The ASCAT-A NOC corrections as used in AWDP are based on a full year and the close proximity of the current ASCAT-A NOC indicates that also the ASCAT-B NOC over the same period would be representative of an ASCAT-B calibration over a full year (which is not yet available). This provides a priori quite some confidence in the early ASCAT-B NOC corrections as described in this report.

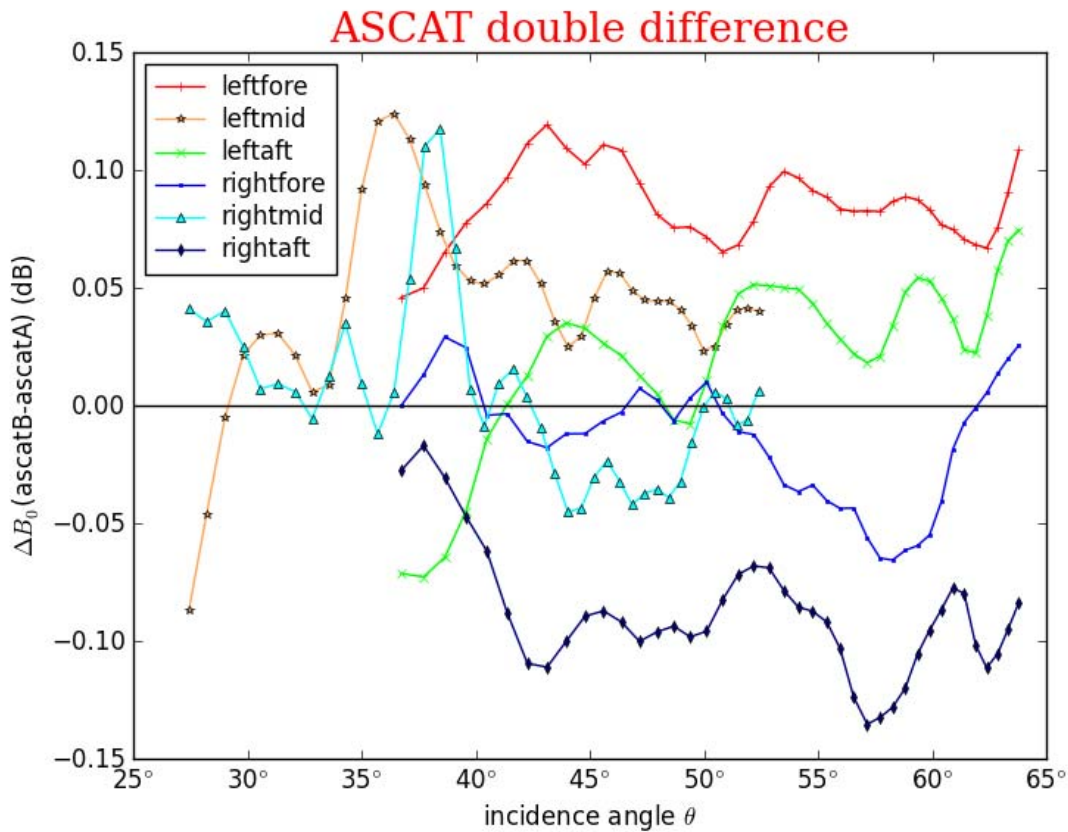
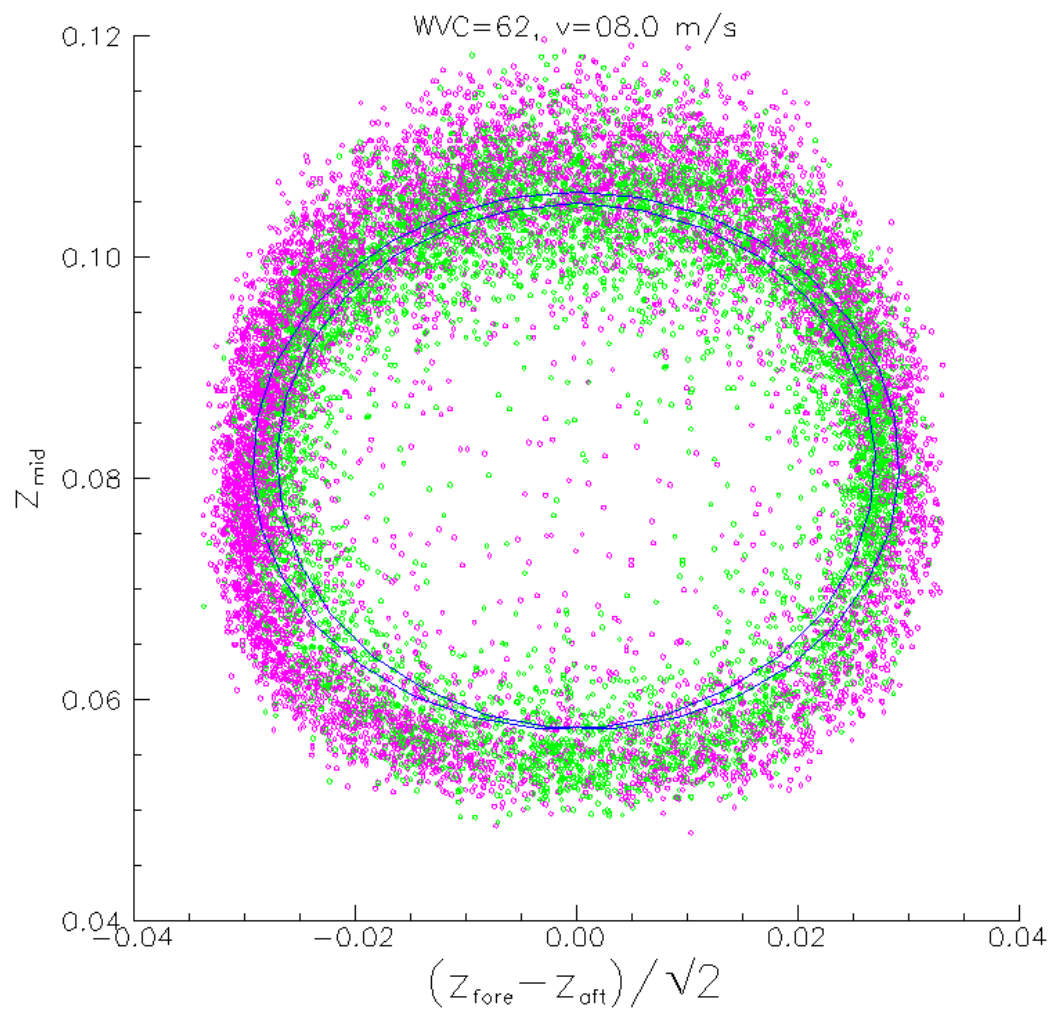


Figure 4 – Double difference of NOC residuals for ASCAT-B and ASCAT-A coastal data from 2012-11-15 to 2012-11-30.

4 Visualisation

Visualisations of the data triplets in measurement space together with the GMF have been made in order to see how well the GMF fits the cloud of measurements. Purple triplets belong to the outer cone surface and green triplets belong to the inner surface. WVC 62 is in the middle of the right swath and has incidence angles fore/aft=58.8°, mid=47.5°. All results in this section are obtained from the coastal wind product.

Figure 5a) shows the cone intersection with the plane $z_{\text{fore}} + z_{\text{aft}} = c$, with the constant c roughly corresponding to a modal wind speed $V=8$ m/s. Data is used with NOC corrections applied. Figure 5b) shows the cone intersection with the $z_{\text{fore}} = z_{\text{aft}}$ plane. Data triplets within a certain small distance of the plane are also shown. Both figures show a good fit.



a)

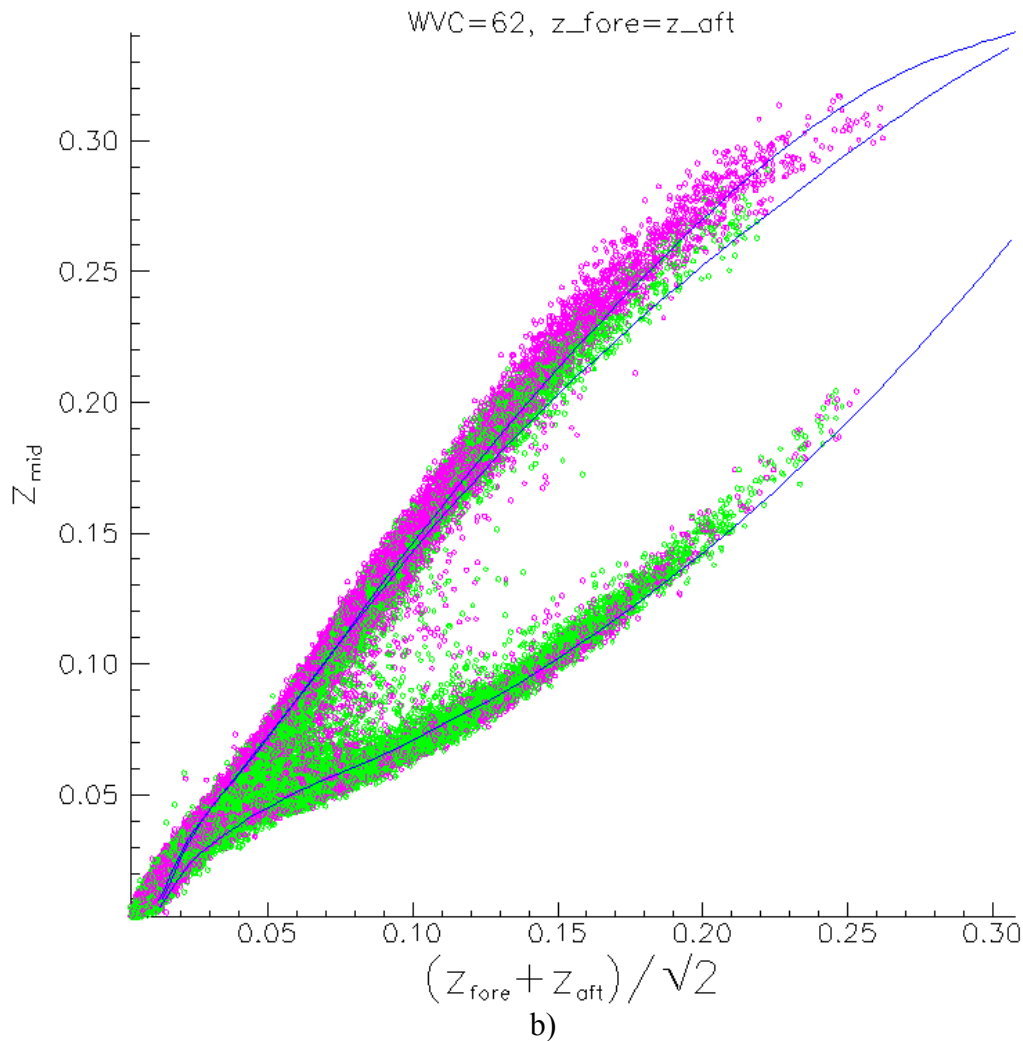


Figure 5 - Visualisation of CMOD5.n for WVC 62 (middle of the right swath), incidence angle fore/aft=58.8°, mid=47.5°) together with data triplets. Purple triplets belong to the outer cone surface, green triplets belong to the inner cone surface. NOC corrections are applied.

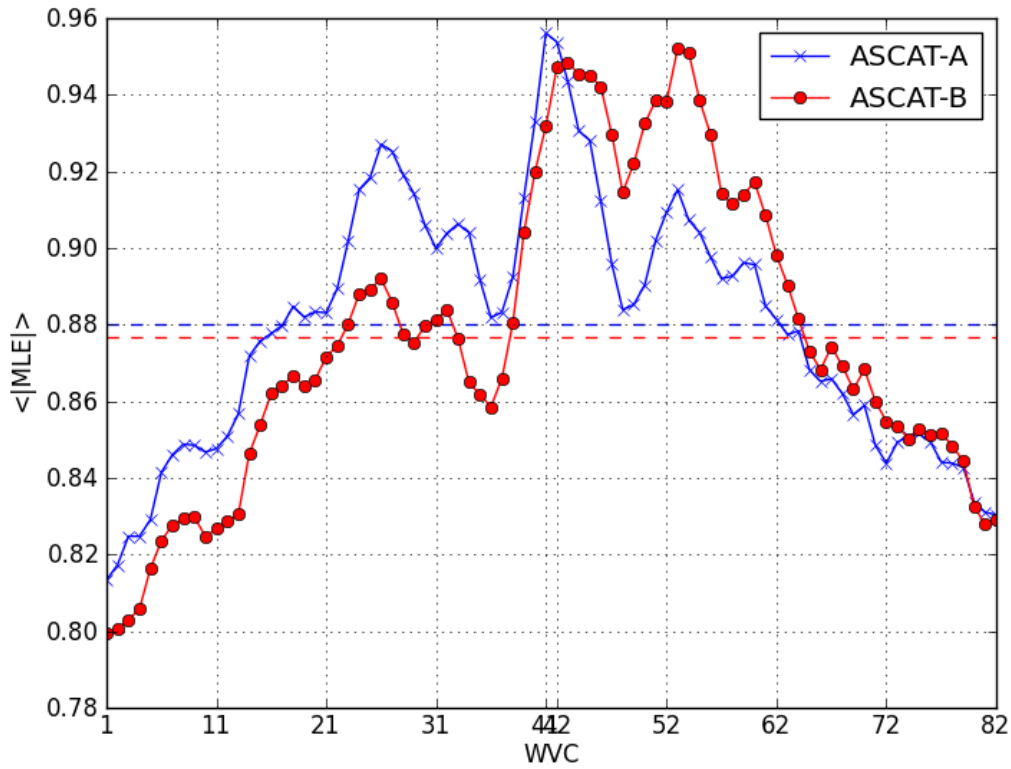
- a) Intersection of the cone with the plane $(z_{fore}+z_{aft})/\sqrt{2} = z_{ref}$. The value of z_{ref} is 0.0730, the z_{mid} value at wind direction $\phi = 0$ and corresponding to a wind speed of $V=8.0$ m/s. Triplets within a distance of $\pm 0.02 z_{ref}$ from the mentioned plane are plotted.
- b) Intersection of the cone with the plane $z_{fore}=z_{aft}$. Triplets within a distance of ± 1.0 dB from the mentioned plane are plotted.

5 MLE

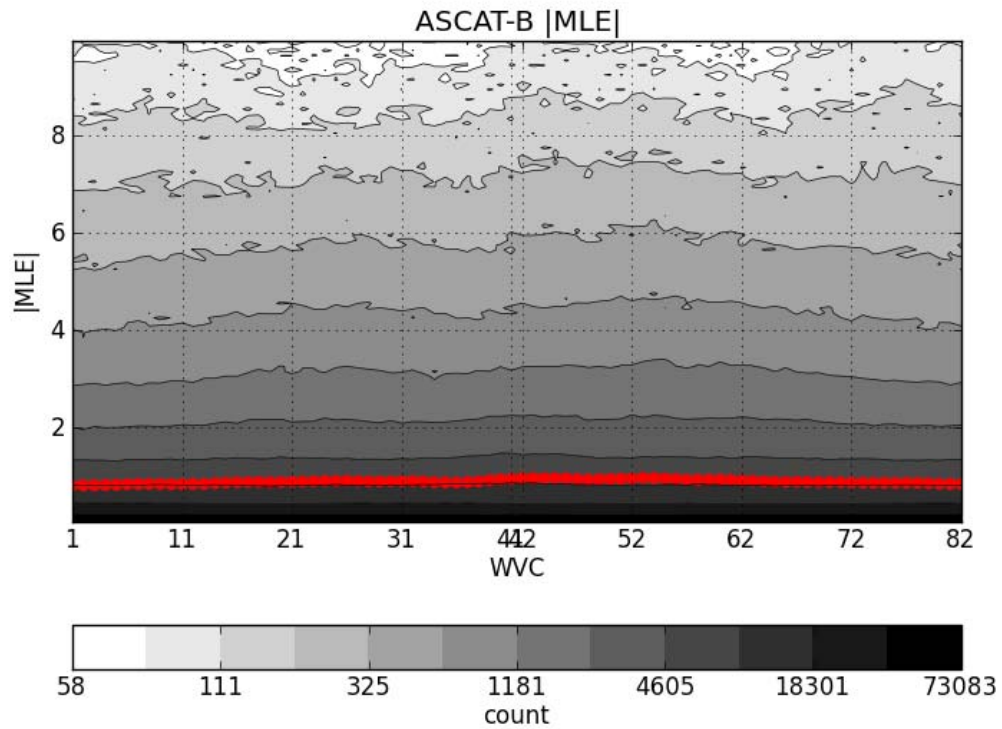
The Maximum Likelihood Estimate (MLE) is the normalised distance in 3D measurement space from a measurement triplet to the point on the wind cone that corresponds to the retrieved wind. It is a measure of how well the measurement and GMF fit to each other. The MLE is normalised using a table in order to get an expectation value of $\langle |MLE| \rangle = 1$ for

each WVC ($\langle |MLE| \rangle$ denotes the average of the absolute value of the MLE). The MLE normalisation table was derived for ASCAT-A and is also used for ASCAT-B.

Figure 6a) and Figure 6b) show the average $|MLE|$ value per WVC for NOC corrected data. The figures for ASCAT-A and ASCAT-B are similar. For both scattermeters the same MLE normalisation table derived from ASCAT-A data is used.



a)



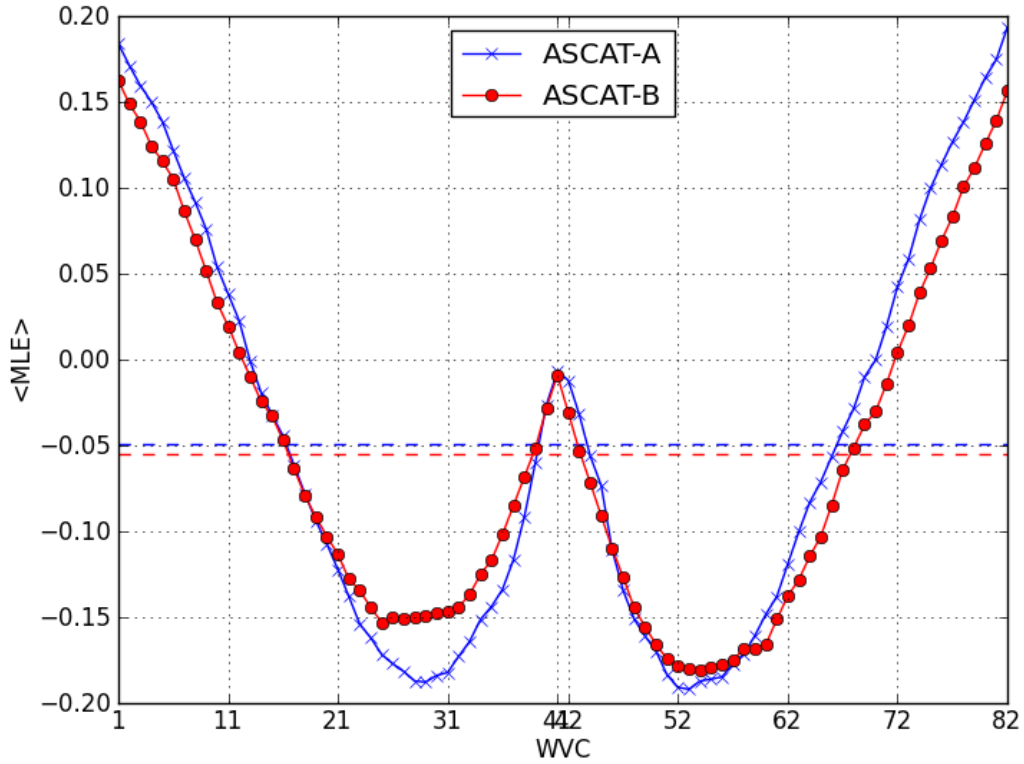
b)

Figure 6 – Absolute value of the MLE per WVC. NOC corrections are applied. Coastal data from 2012-11-15 to 2012-11-30 is used.

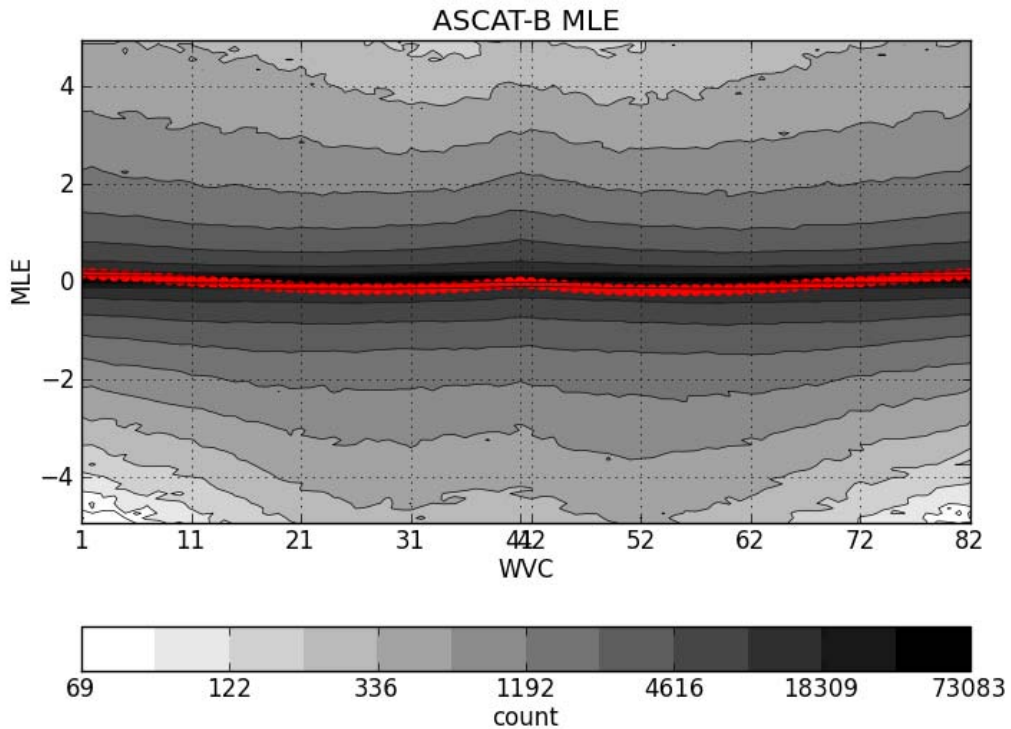
a) Average |MLE| per WVC for ASCAT-A and ASCAT-B. The values averaged over all WVCs are shown as dashed lines.

b) Contour plot of the ASCAT-B |MLE| with average value in red.

Figure 7a) and Figure 7b) show the MLE value (not the absolute value) per WVC for NOC corrected data. The figure for ASCAT-B is again similar to the figure for ASCAT-A. There is a small dependency left of the MLE expectation value on WVC number/incidence angle.



a)



b)

Figure 7 – Value of the MLE per WVC. NOC corrections are applied. Coastal data from 2012-11-15 to 2012-11-30 is used.

a) Average MLE per WVC for ASCAT-A and ASCAT-B. The values averaged over all WVCs are shown as dashed lines.

b) Contour plot of the ASCAT-B MLE with average value in red.

Figure 8 shows the $\langle |MLE| \rangle$ and $\langle MLE \rangle$ per WVC for the 25 km WVC spacing product of ASCAT-A and ASCAT-B. These Hamming-window filtered data show the same characteristics and absolute values as their 12.5 km coastal product counterparts.

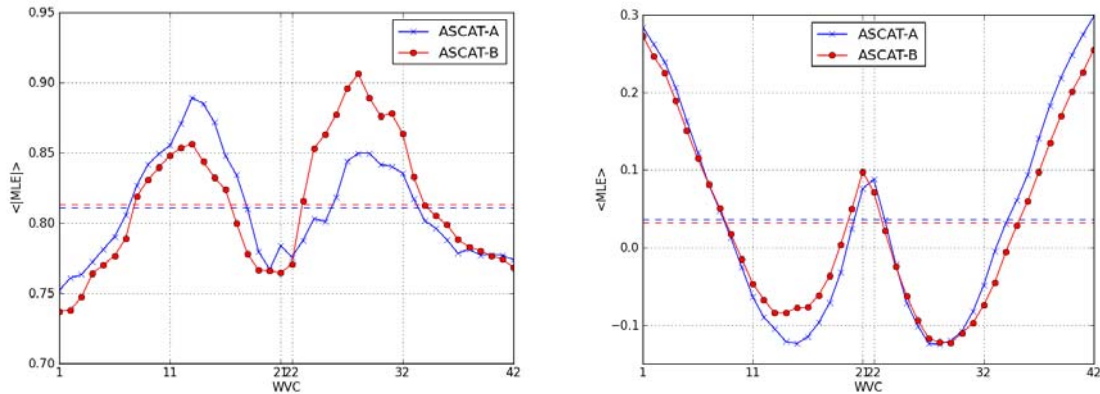


Figure 8 - Value of $\langle |MLE| \rangle$ on the left and $\langle MLE \rangle$ on the right. NOC corrections are applied. 25-km WVC spacing data (Hamming-window filtered) is used from 2012-11-15 to 2012-11-30.

6 Wind statistics

The wind speed statistics based on the scatterometer wind and the NWP wind (corrected to neutral wind) as a function of WVC is calculated with NOC corrections applied. The scatterometer wind direction skill is very low for low wind speeds. Therefore only NWP wind speeds above 4 m/s are considered for wind direction statistics.

In Figure 9 contour plots of the wind speed, wind direction and also the zonal and meridional wind components u and v are shown of ASCAT-B versus ECMWF. For high winds ($V > 20$ m/s) the scatterometer wind is somewhat biased high with respect to the NWP wind. This deviation is not observed for ASCAT-A over the same period. Because the number of high winds is so low it does not have a significant influence on overall statistics. This issue needs some further investigation. Apart from this, the plots show symmetrical results.

ASCAT-B

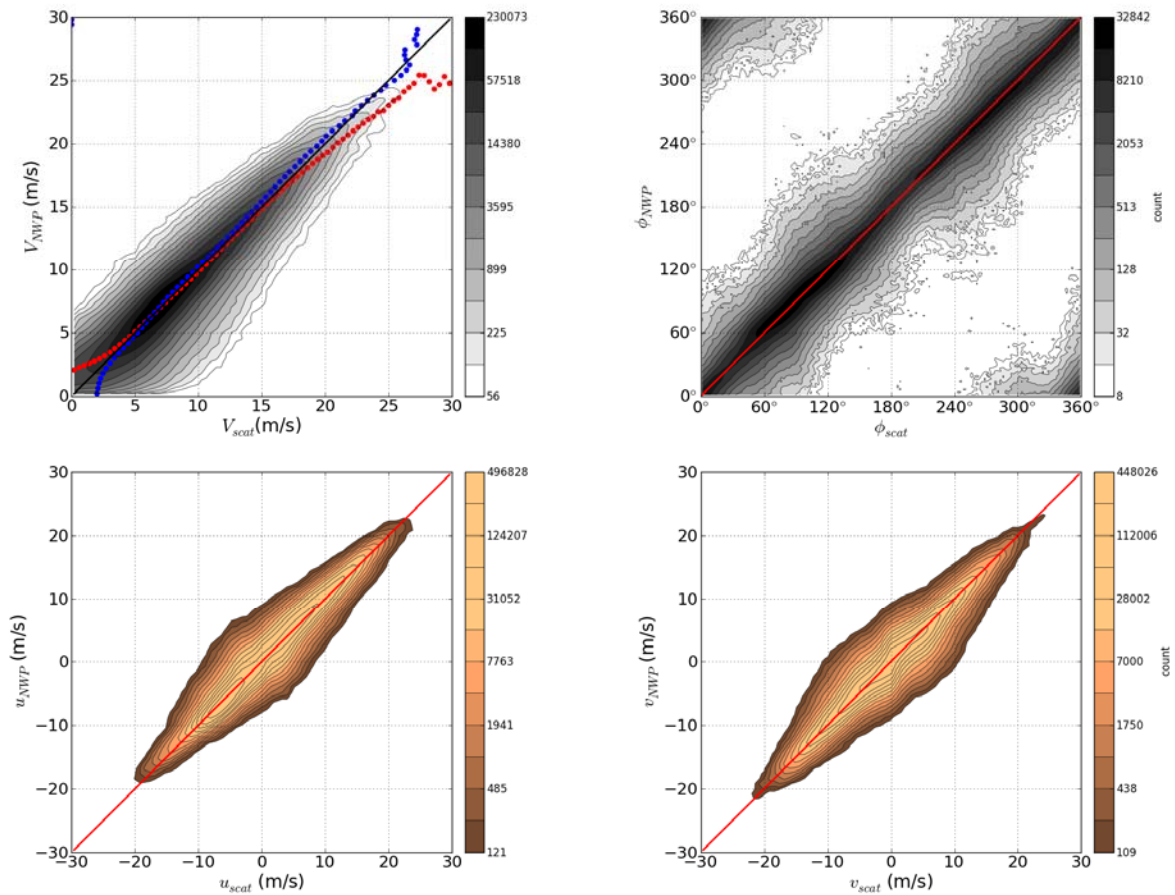


Figure 9 – Contour plots of the wind speed, wind direction, and the u and v components of (ASCAT-B-ECMWF). NOC corrections are applied. Coastal data from 2012-11-15 to 2012-11-30 is used.

In Figure 10 the averaged wind speed and wind direction difference between ASCAT-B and ECMWF are shown on the left. Also their respective SDs are shown on the right. The patterns are symmetric for the left and right swath and similar to figures for ASCAT-A.

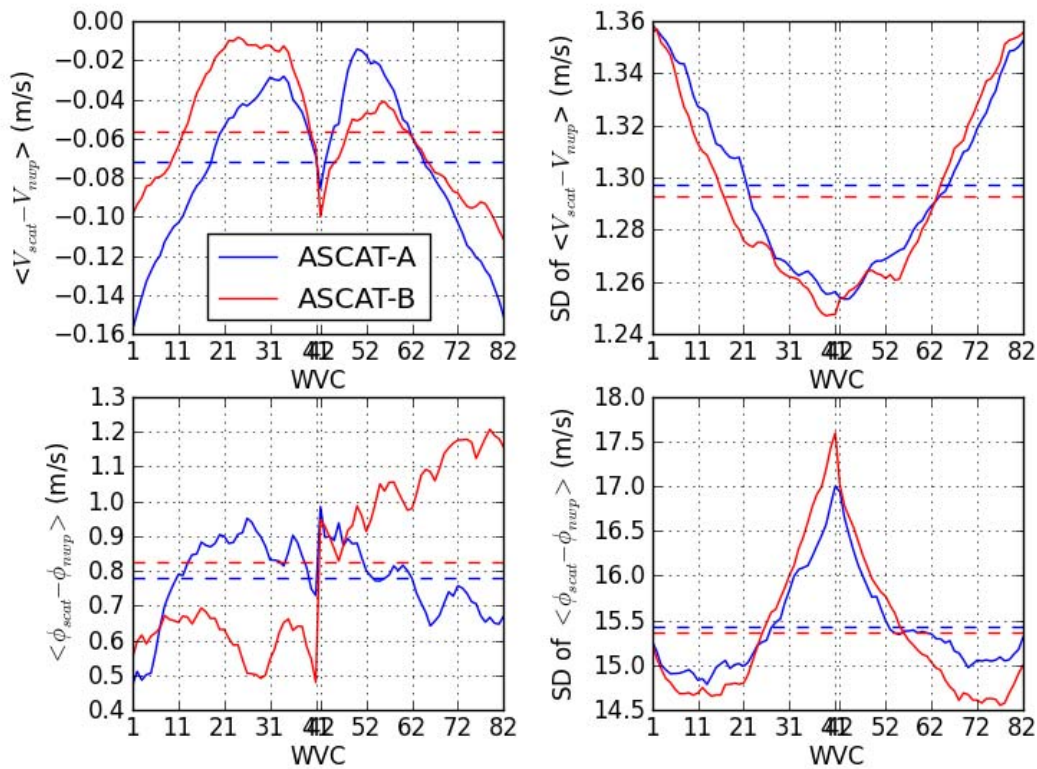


Figure 10 – Averaged differences of (ASCAT-ECMWF) wind speed and wind direction and their standard deviation as a function of WVC from 2012-11-15 to 2012-11-30 for both ASCAT-A and ASCAT-B. NOC corrections are applied. The dashed lines show the value averaged over all WVCs.

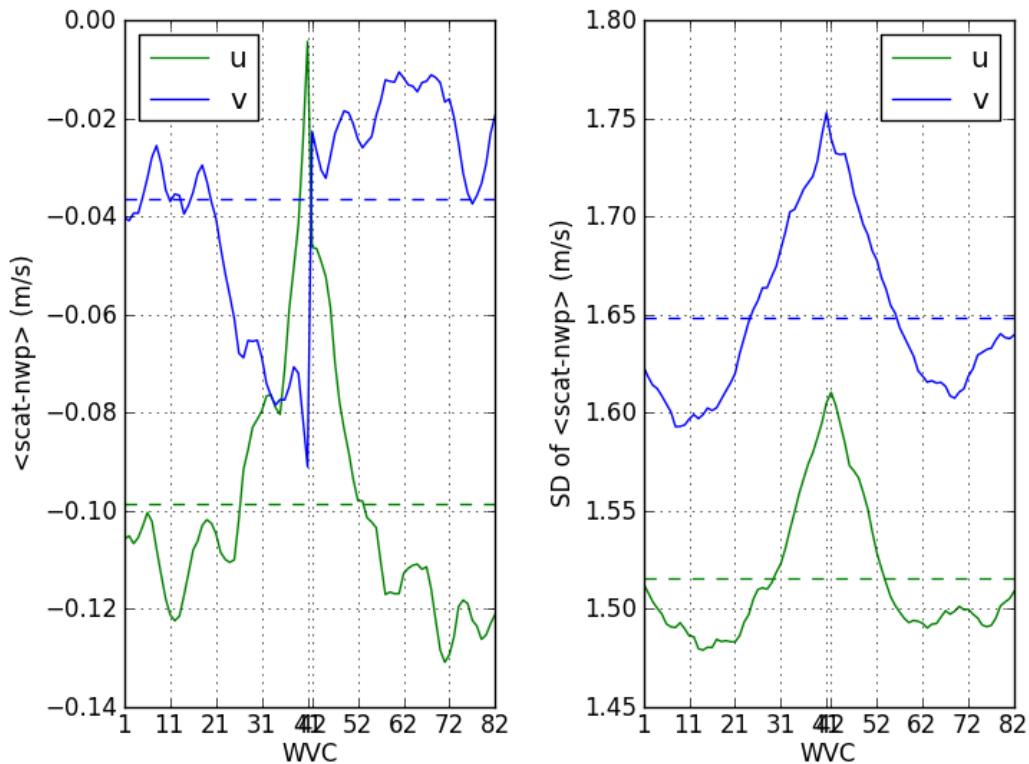


Figure 11 – Averaged differences of (ASCAT-ECMWF) u and v wind components and SD as a function of WVC. NOC corrections are applied. The dashed lines show the value averaged over all WVCs. Coastal data from 2012-11-15 to 2012-11-30 is used.

In Figure 11 the averaged wind vector component differences between ASCAT-B and ECMWF are shown on the left. Their respective SDs are shown on the right. Again the patterns are symmetric and similar to figures for ASCAT-A. Table 1 (coastal product) and Table 2 (25.0 km product) summarise the wind statistics for ASCAT-B and show the ASCAT-A numbers for comparison. For ASCAT-A exactly the same conditions as for ASCAT-B were used.

Table 1 – Wind statistics for ASCAT-A and ASCAT-B from 2012-11-15 to 2012-11-30, coastal product.

	<scatB-nwp>	SD	<scatA-nwp>	SD
V (m/s)	-0.06	1.29	-0.07	1.29
ϕ	0.8°	15.4°	0.8°	15.4°
u (m/s)	-0.10	1.52	-0.09	1.52
v (m/s)	-0.04	1.65	-0.04	1.65

Table 2 – Wind statistics for ASCAT-A and ASCAT-B from 2012-11-15 to 2012-11-30, 25 km product.

	<scatB-nwp>	SD	<scatA-nwp>	SD
V (m/s)	-0.06	1.22	-0.08	1.22
ϕ	0.9°	14.1°	0.9°	14.2°
u (m/s)	-0.11	1.43	-0.11	1.44
v (m/s)	-0.03	1.54	-0.04	1.54

7 Quality control

The occurrence ratio of some important level 2 quality flags and their WVC dependency is shown in Figure 12 for ASCAT-A and ASCAT-B. The GMF distance flag is set when the measured triplet has an anomalously large distance to the GMF cone, while the var_qc flag is set during 2DVAR ambiguity removal when a wind vector is spatially inconsistent with its neighbours. All fractions are low and comparable for ASCAT-A and ASCAT-B.

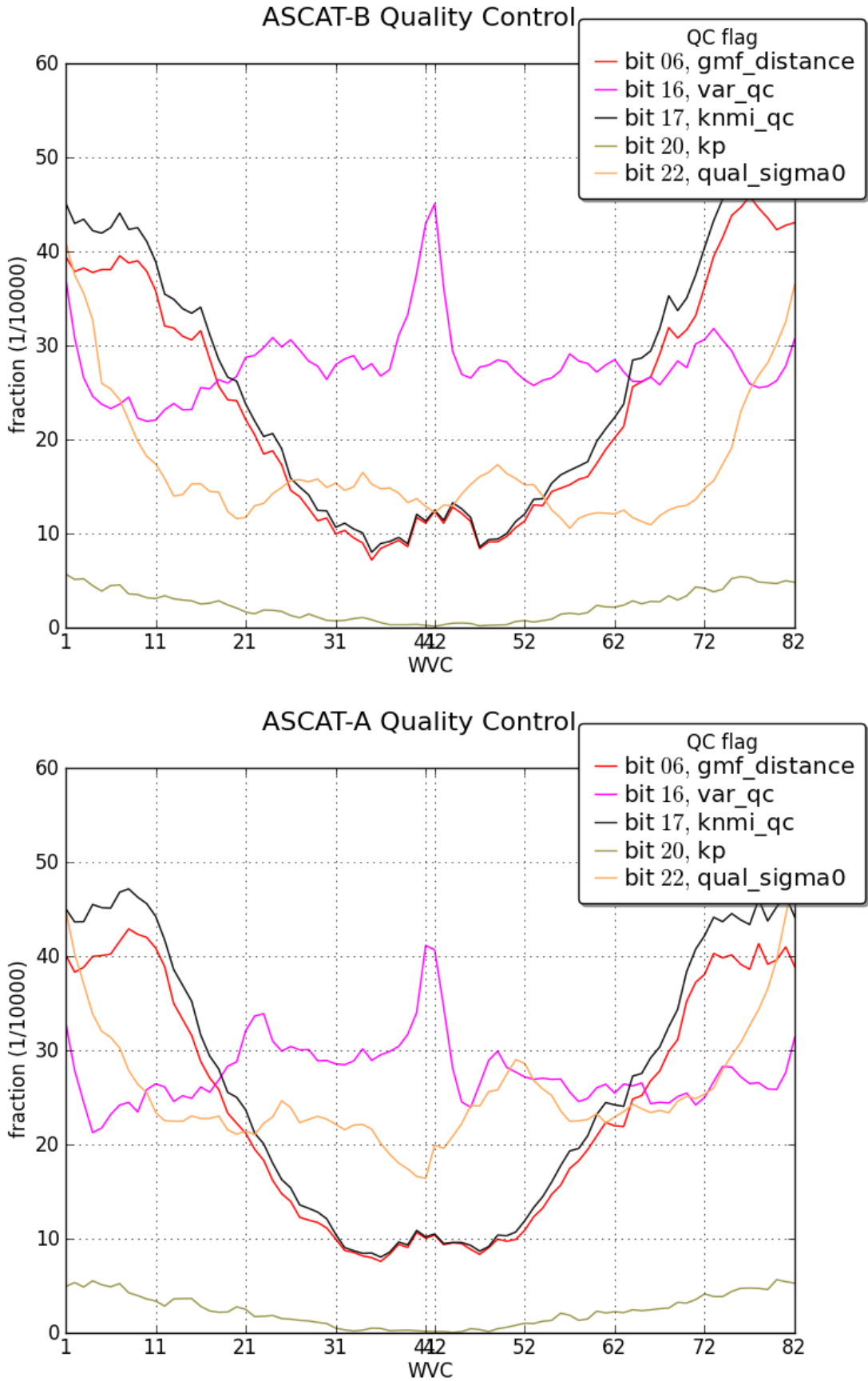


Figure 12 – Some level 2 quality flag occurrence ratios as a function of WVC. NOC corrections are applied. Top ASCAT-B, bottom ASCAT-A.

Figure 13 shows the monitoring of the $\langle \text{MLE} \rangle$ and the average wind speed difference $\langle V_{\text{scat}} - V_{\text{nwp}} \rangle$ from the development status near-real time wind processing of ASCAT-B around the introduction of the NOC corrections on 12 November 2012 (Note: the level 2 ASCAT-B data stored at KNMI has been reprocessed with the NOC corrections from the launch of Metop-B to 12 November 2012 in order to get a consistent record). The data is divided into six WVC groups for the inner, middle and outer regions of the left and right swath. Especially for the outer swath groups the effect of the NOC corrections is clearly visible as a reduced $\langle \text{MLE} \rangle$ and a reduced average wind speed difference.

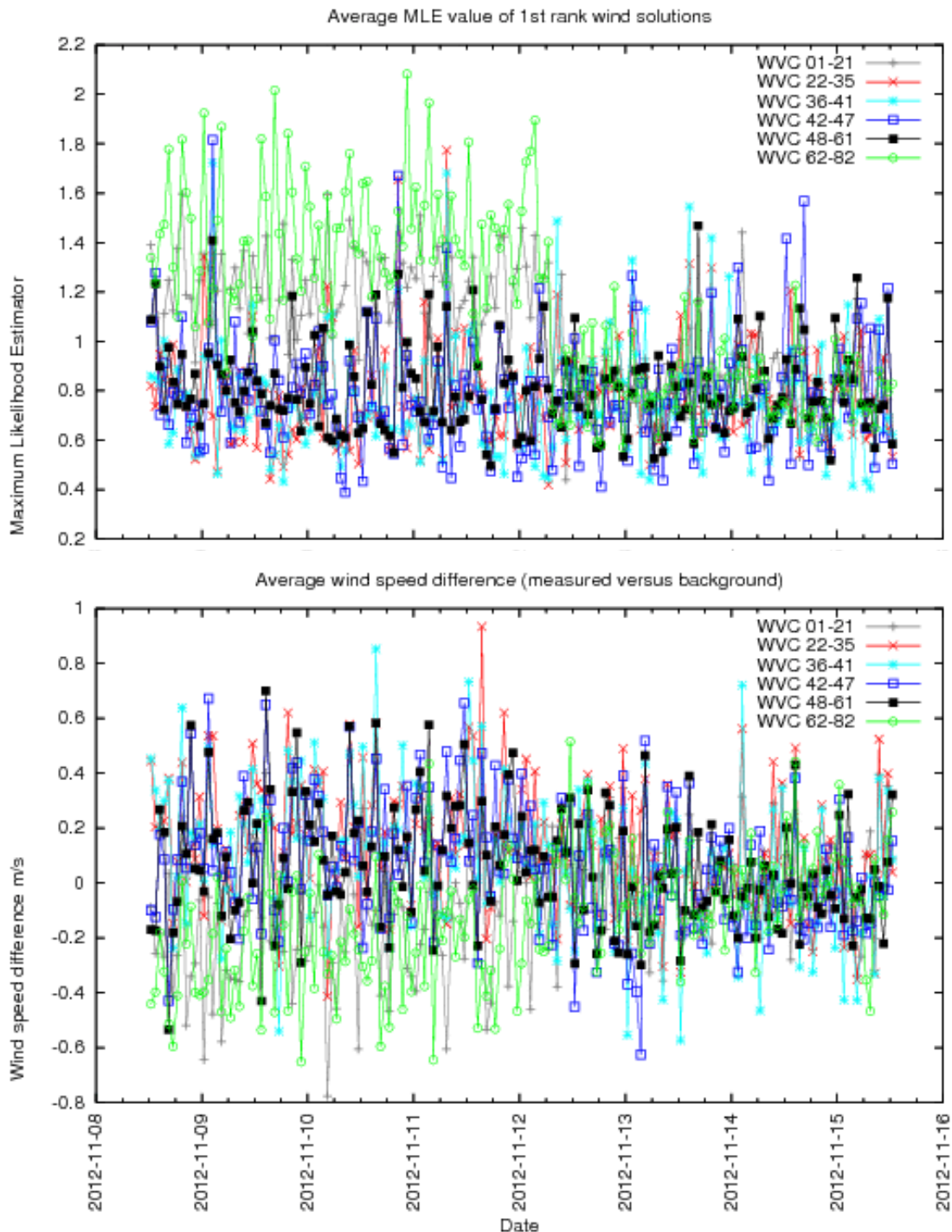


Figure 13 – AWDP MLE and wind speed bias monitoring of ASCAT-B around the introduction of the ASCAT-B NOC corrections on 12 Nov. 2012.

8 ASCAT-A and ASCAT-B collocation

The simultaneous operation of Metop-A and Metop-B leads to an increased (short term) spatial coverage for the ASCAT-A and ASCAT-B constellation when compared to the coverage of ASCAT-A alone. The exact coverage depends amongst others on the phasing that is chosen for Metop-B with respect to Metop-A. The chosen phasing is a 48.93 minute delay which may be compared to the 101.36 minute orbit duration. Both satellites are in the same 9:30 LST morning orbit (Local Time of Descending Node) and thus almost half an orbit (173.79°) apart.

Figure 14 shows the collocation histogram for ASCAT-A and ASCAT-B for data from 2012-11-01 to 2012-11-14. The maximum distance between collocated WVCs is 10 km. As a time filter a 6 minute window around the delay time of 48.93 minute is taken (ASCAT-A ahead of ASCAT-B). Other collocations occur at a delay time of 52.43 minutes (ASCAT-B ahead of ASCAT-A) but these are not taken into account here.

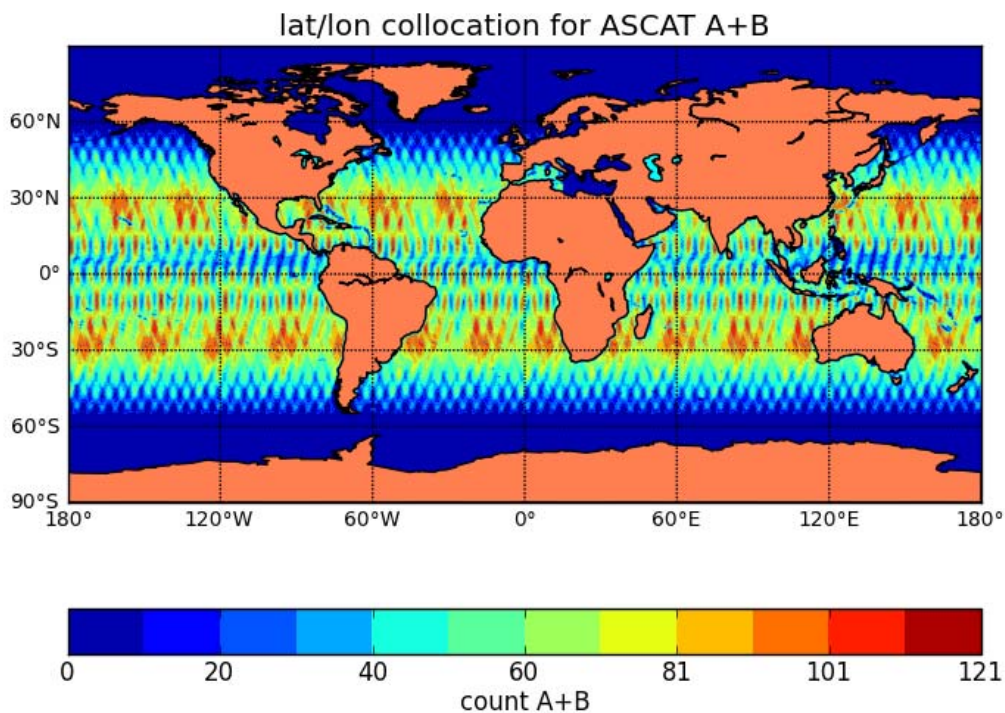


Figure 14 – Collocation for ASCAT-A and ASCAT-B. Maximum distance between WVCs is 10 km. Time difference is 48.93 minutes with a 6 minute time window. ASCAT data is used from 2012-11-01 to 2012-11-14.

Figure 15 shows the wind speed and wind direction histograms for ASCAT-A versus ASCAT-B for the scatterometer data on the left and the NWP data on the right. All graphs are highly symmetric and show a high correlation. Asymmetry could indicate deficiencies in one of the instruments. The NWP plots have a higher correlation than the scatterometer plots. This is not caused by the fact that the NWP model would have a smaller error in the wind vector than the scatterometer. In fact from triple collocation studies it follows that the scatterometer error is smaller than the NWP model error [Vogelzang et al, 2011]. The apparently smaller error is caused by the fact that the collocated NWP wind vectors from ASCAT-A and ASCAT-B are highly dependent. If we had perfect collocations in time and space, the NWP winds would be completely dependent with correlation coefficient $R=1$ (both satellites would have the same collocated NWP wind). The correlation coefficient for scatterometer winds would be less than unity ($R<1$) because the measurement of the same wind by both satellites would be completely independent.

Because of the low scatterometer wind direction skill for low wind speeds only NWP wind speeds above 4 m/s are considered for wind direction statistics. The scatterometer wind direction contour plot shows some side lobes which are caused by imperfections in the wind retrieval and ambiguity removal.

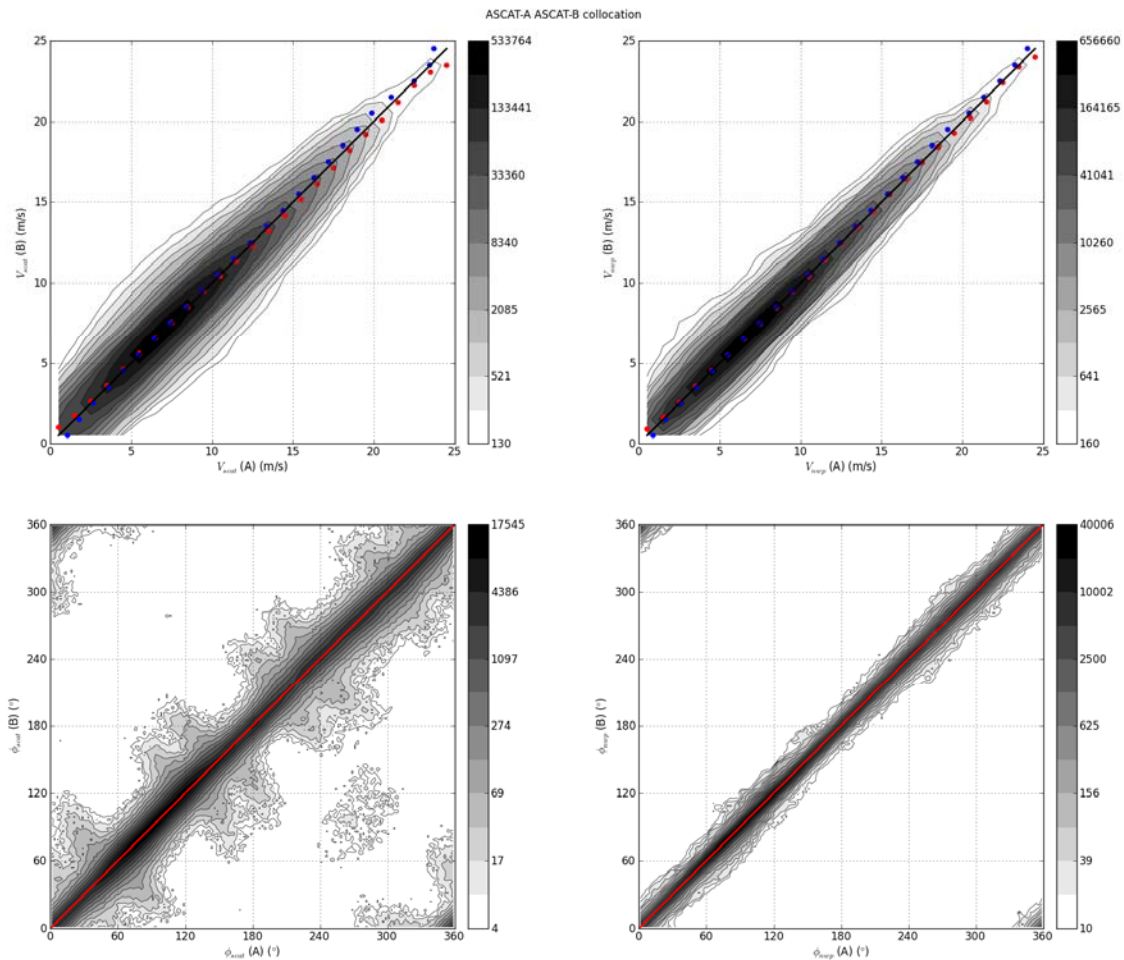


Figure 15 – Wind speed and wind direction PDF for the collocated ASCAT-A and ASCAT-B data. Maximum distance between WVCs is 10 km. Time difference is 48.93 minutes with a 6 minute time window. ASCAT coastal data is used from 2012-11-01 to 2012-11-14.

The high-wind ($s > 20$ m/s) bias of ASCAT-B w.r.t. ECMWF noted in Figure 9 and which does not appear over the same period in ASCAT-A appears a sampling issue, since winds above 20 m/s are evident in Figure 15 for both the ASCAT-A/B and ECMWF panels, but no bias is apparent in either.

9 Buoy validation and triple collocations

In this section, scatterometer wind data are compared with in situ buoy wind measurements. The buoy winds are distributed through the Global Telecommunication System (GTS) and have been retrieved from the ECMWF MARS archive. The buoy data are quality controlled and (if necessary) blacklisted by ECMWF [Bidlot et al. 2002]. We used a set of approximately 150 moored non-coastal buoys spread over the oceans (most of them in the tropical oceans and near Europe and North America) which are also used in the buoy validations that are routinely performed for the OSI SAF wind products (see the links on <http://www.knmi.nl/scatterometer/osisaf/>). Most of these buoys are located more than 50 kilometres from the coast.

See Figure 16 for the locations of the buoys used in the comparisons. A scatterometer wind and a buoy wind measurement are considered to be collocated if the distance between the Wind Vector Cell (WVC) centre and the buoy location is less than the WVC spacing divided by $\sqrt{2}$ and if the acquisition time difference is less than 30 minutes.

The buoy winds are measured hourly by averaging the wind speed and direction over 10 minutes. The real winds at a given anemometer height have been converted to 10 m equivalent neutral winds using the LKB model [Bidlot et al. 2002], [Liu et al. 1979] in order to enable a good comparison with the 10 m scatterometer winds.

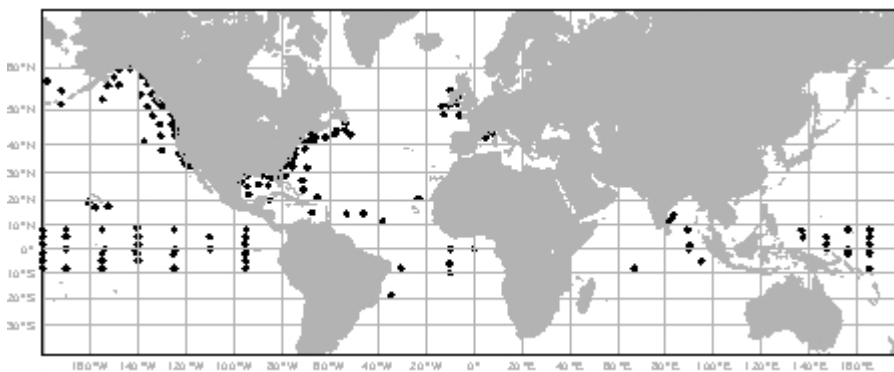


Figure 16 – Locations of the moored buoys used in the comparisons.

In Table 3 we compare the ASCAT-A and ASCAT-B buoy collocations for the period of 1 November 2012 to 31 January 2013 (3 months). It is clear from the results that ASCAT-A and ASCAT-B have comparable quality. We observe that the coastal products have more collocations than the 25-km products: some buoys are on locations in the vicinity of land where the 25-km products will not yield collocations. Also differences in quality control between the 25-km and coastal products may cause different collocation amounts.

The detailed buoy collocation results in terms of wind speed, wind direction and wind components for the 25-km wind products are shown in Figure 17. It is clear that ASCAT-A and ASCAT-B have quite similar characteristics.

	# wind vectors	speed bias	stdev u	stdev v
ASCAT-A 25-km	6257	-0.02	1.72	1.76
ASCAT-B 25-km	6280	0.05	1.78	1.80
ASCAT-A Coastal	7710	0.01	1.73	1.85
ASCAT-B Coastal	7623	0.08	1.76	1.80

Table 3 – Buoy collocation results of ASCAT-A and ASCAT-B wind products from November 2012 to January 2013.

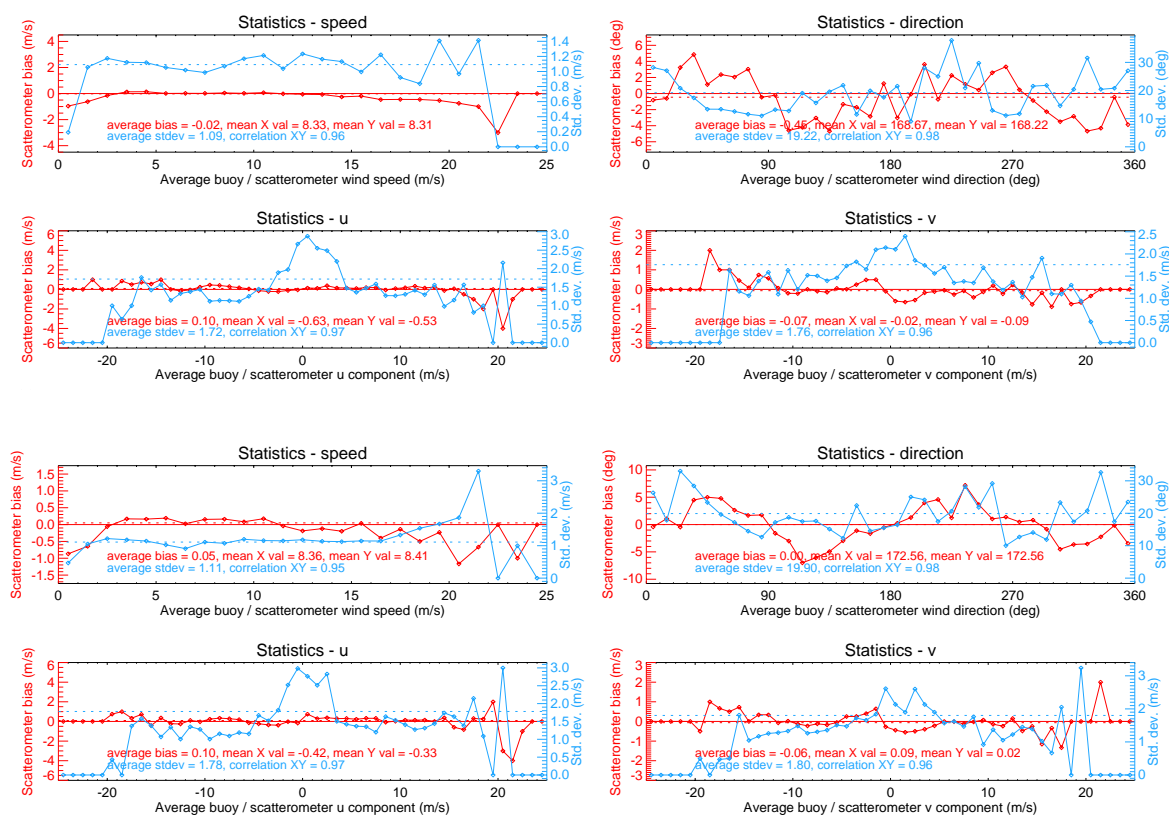


Figure 17 – Biases of wind speed, direction (w.r.t. wind coming from the North), u and v components of ASCAT-A (top) and ASCAT-B (bottom) 25-km wind products versus the buoy winds from November 2012 to January 2013. The biases (red) and standard deviations (blue) as a function of the average scatterometer and model winds are shown.

A triple collocation study was performed to assess the errors of the ASCAT, ECMWF and buoy winds independently. The triple collocation method was introduced by [Stoffelen 1998]. Given a set of triplets of collocated measurements and assuming linear calibration, it is possible to simultaneously calculate the errors in the measurements and the relative calibration coefficients. The triple collocation method can give the measurement errors from the coarse resolution NWP model perspective or from the intermediate resolution scatterometer perspective, but not from the fine resolution buoy perspective without further assumptions on the local buoy measurement error. A wind signal present in buoy measurements but not in scatterometer measurements is therefore contained in the buoy

error. This matter is introduced in [Stoffelen 1998] and extensively discussed in [Vogelzang et al. 2011].

Collocated data sets of ASCAT-A 25-km, ASCAT-B 25-km, ASCAT-A coastal and ASCAT-B coastal with ECMWF and buoy winds spanning three months were used in the triple collocation. Table 4 lists the error variances of the buoy, ASCAT and ECMWF winds from the intermediate resolution scatterometer perspective. The precision of the scatterometer error standard deviations is approximately 0.03 m/s, assuming that the error is Gaussian and that the representation error is known. For buoys, the precision estimation is 0.05 m/s and for ECMWF, this is 0.04 m/s.

Table 4 shows that the ASCAT-A and ASCAT-B 25 km products give the same errors in scatterometer, buoys, and ECMWF background within the precision given above. The same applies to the ASCAT-A and ASCAT-B coastal products. The errors in Table 4 are with respect to the scatterometer, so the representation error, calculated from the difference between scatterometer and ECMWF spectra, are attributed to the ECMWF background. Therefore the ECMWF errors are larger for the coastal products than for the 25 km products. Similarly, the common variance between buoys and coastal product should be larger than between buoys and 25-km product, leading to smaller buoy errors in the former comparison, but this effect disappears within the significance error. Finally, note that coastal winds are more variable than open ocean winds, thus resulting in larger total error variances (i.e., the sum of buoy, scatterometer and ECMWF).

The scatterometer standard deviations for ASCAT-A and ASCAT-B are equal for each product within the expected ± 0.03 m/s so we conclude that there are no significant differences between the ASCAT-A and ASCAT-B winds found by the triple collocation study.

	Scatterometer		Buoys		ECMWF	
	σ_u (m/s)	σ_v (m/s)	σ_u (m/s)	σ_v (m/s)	σ_u (m/s)	σ_v (m/s)
ASCAT-A 25-km	0.63	0.71	1.21	1.35	1.39	1.44
ASCAT-B 25-km	0.63	0.66	1.26	1.39	1.38	1.42
ASCAT-A Coastal	0.76	0.84	1.18	1.34	1.54	1.57
ASCAT-B Coastal	0.81	0.79	1.24	1.35	1.53	1.57

Table 4 – Error standard deviations from triple collocation of ASCAT wind products with buoy and ECMWF forecast winds, seen from the scatterometer perspective. The results were obtained for the period of November 2012 to January 2013.

10 Conclusions

On September 17, 2012 the Metop-B satellite with onboard the Advanced Scatterometer (ASCAT-B) has been successfully launched. Following established procedures for ASCAT-A, for the ASCAT-B scatterometer corrections are derived with the use of NWP ocean calibration (NOC). These corrections are subsequently used in the ASCAT wind data processor (AWDP) with the objective to obtain high-quality winds. The NOC-calibrated

ASCAT-B wind product is examined and its quality appears on the same level as that of the ASCAT-A wind product.

The NOC corrections for ASCAT-B are derived and used in the ASCAT-B operational wind processing for both the 12.5-km WVC-spacing coastal product and the 25-km WVC-spacing product. As for ASCAT-A, the characteristics of the 25 km product and the 12.5 km coastal product are very similar but with more spatial detail in the higher resolution product, as expected. ASCAT-B gives results that are comparable with ASCAT-A for all examined parameters: ocean calibration, MLE, wind vector quality statistics and quality flagging.

Whereas a bias appears for ASCAT-B against ECMWF at high wind speeds ($s > 20$ m/s) the scatterometer winds from ASCAT-A are not biased against ECMWF over the same period (not shown). This ASCAT-B effect appears due to sampling as no biases appear at high winds for collocated ASCAT-A and ASCAT-B winds. Generally, collocated ASCAT-A and ASCAT-B data (49 minutes apart) show no large asymmetries and low noise.

Buoy collocations and a triple collocation study show that there are no significant differences in wind quality between the ASCAT-A and ASCAT-B wind products. ASCAT-B appears a successful successor of ASCAT-A and the user community may look forward to an interesting period of tandem ASCAT-A and ASCAT-B winds of high quality.

Glossary

ASCAT	- Advanced SCATterometer
AWDP	- ASCAT Wind Data Processor
ECMWF	- European Centre for Medium-range Weather Forecast
ERS	- European Remote-Sensing satellite
GMF	- Geophysical Model Function
MLE	- Maximum Likelihood Estimate
NOC	- NWP-based OC
NWP	- Numerical Weather Prediction
OC	- Ocean Calibration
SAF	- Satellite Application Facility
SD	- Standard Deviation
WVC	- Wind Vector Cell
QC	- Quality Control

References

[ASCAT user manual] A. Verhoef and A. Stoffelen, ASCAT Wind Product User Manual version 1.8, SAF/OSI/CDOP/KNMI/TEC/MA/126, EUMETSAT, 2010.

[Attema 1991] Attema, E.P.W., "The Active Microwave Instrument on-board the ERS-1 satellite," Proceedings of the IEEE , vol.79, no.6, pp.791-799, Jun 1991
doi: 10.1109/5.90158

[Bidlot et al. 2002] Bidlot J., D. Holmes, P. Wittmann, R. Lalbeharry, and H. Chen, Intercomparison of the performance of operational ocean wave forecasting systems with buoy data, Wea. Forecasting, vol. 17, 287-310, 2002

[EUMETSAT 2005] "ASCAT Product Generation Function Specification", EUM.EPS.SYS.SPE.990009, Issue 6 rev 6, Darmstadt Germany, April 11, 2005

[Figa-Saldaña et al 2002] Figa-Saldaña, J., J.J.W. Wilson, E. Attema, R. Gelsthorpe, M.R. Drinkwater, and A. Stoffelen, The Advanced scatterometer (ASCAT) on the meteorological operational (MetOp) platform: A follow on for the European wind scatterometers, Can. J. Remote Sensing **28** (3), pp. 404-412, 2002.

[Hersbach 2010] H. Hersbach, "CMOD5.N: Comparison of C-band scatterometer CMOD5.n equivalent neutral winds with ECMWF", J. Atmos. Oceanic Technol., 27, 721–736, 2010, doi: 10.1175/2009JTECHO698.1

[KNMI site]

http://www.knmi.nl/scatterometer/ascat_osi_25_prod/ascat_app.cgi?cmd=buoy_validations

[Liu et al. 1979] Liu, W.T., K.B. Katsaros, and J.A. Businger, Bulk parameterization of air-sea exchanges of heat and water vapor including the molecular constraints in the interface, *J. Atmos. Sci.*, vol. 36, 1979.

[Portabella and Stoffelen 2009] Portabella, M., and Stoffelen, A., 2009, "On scatterometer ocean stress". *J. Atmos. Oceanic Technol.*, 26, 368–382, doi: <http://dx.doi.org/10.1175/2008JTECHO578.1>

[Portabella et al 2012] Portabella, M.; Stoffelen, A.; Wenming Lin; Turiel, A.; Verhoef, A.; Verspeek, J.; Ballabrera-Poy, J.; , "Rain Effects on ASCAT-Retrieved Winds: Toward an Improved Quality Control," *Geoscience and Remote Sensing, IEEE Transactions on* , vol.50, no.7, pp.2495-2506, July 2012, doi: 10.1109/TGRS.2012.2185933

[Stoffelen and Anderson 1997] Stoffelen, Ad, and Anderson, David, "Scatterometer Data Interpretation: Measurement Space and inversion", *J. Atm. and Ocean Techn.*, 14(6), 1298-1313, 1997.

[Stoffelen 1998] Stoffelen, A., Toward the true near-surface wind speed: error modelling and calibration using triple collocation, *J. Geophys. Res.* 103C4, 7755-7766, 1998.

[Stoffelen 1999] Stoffelen, A., "A Simple Method for Calibration of a Scatterometer over the Ocean", *J. Atm. and Ocean Techn.* 16(2), 275-282, 1999.

[Verspeek 2006] Verspeek, Jeroen, "Scatterometer calibration tool development", EUMETSAT Technical Report SAF/OSI/KNMI/TEC/RP/092, *KNMI*, de Bilt, 2006

[Verspeek 2008] Jeroen Verspeek, Marcos Portabella, Ad Stoffelen, Anton Verhoef, Calibration and Validation of ASCAT Winds, SAF/OSI/KNMI/TEC/TN/163, *KNMI*, 2008.

[Verspeek et al 2012] J. Verspeek et al (2012) "Improved ASCAT Wind Retrieval Using NWP Ocean Calibration", *IEEE Transactions on Geoscience and Remote Sensing*, vol 50, pp 2488 - 2494, doi: 10.1109/TGRS.2011.2180730.

[Vogelzang et al. 2011] Vogelzang, J., A. Stoffelen, A. Verhoef, and J. Figa-Saldaña (2011), On the quality of high-resolution scatterometer winds, *J. Geophys. Res.*, 116, C10033, doi:10.1029/2010JC006640.